

Neutron production from thermonuclear reactions in laser-generated plasmas

Yuanbin Wu^{1,*}

¹*Max-Planck-Institut für Kernphysik, Saupfercheckweg 1, D-69117 Heidelberg, Germany*

(Dated: January 28, 2019)

The production of intense neutron beams via thermonuclear reactions in laser-generated plasmas is investigated theoretically. So far, state-of-the-art neutron beams are produced via laser-induced particle acceleration leading to high-energy particle beams that subsequently interact with a secondary target. Here we show that neutron beams of similar intensity and two orders of magnitude narrower bandwidth can be obtained from thermonuclear reactions in plasmas generated by Petawatt-class lasers. We study to this end the reaction ${}^2\text{H}(d, n){}^3\text{He}$ in plasmas generated by Petawatt-class laser interacting with D_2 gas jet targets and CD_2 solid-state targets. The use of CD_2 solid-state targets can also allow the direct measurement of the nuclear reaction rates at low temperatures and show great enhancement on the plasma screening comparing to the case of D_2 gas jet targets, opening new possibilities to study these two so far unsolved issues in the field of astrophysics.

Thermonuclear reactions occur in plasma environments in which the thermal energy of the ions can overcome the electrostatic repulsion in a collision between nuclei, leading to nuclear reactions [1]. The development of laser technology in the past decades provides a powerful tool for the study of nuclear reactions in laser-generated plasmas. As plasma is the most abundant form of matter in the universe, the latter provides the opportunity to access parameter regimes which can not be accessed in accelerator-based experiments, such as the direct measurements of nuclear reactions in nucleosynthesis-relevant energies and the role of the plasma effects on nuclear reactions [2–5], and might thus significantly advance our understanding of astrophysical environments. On the other hand, industrial applications of such studies, such as laser-induced ignition which makes fusion energy a viable alternative energy source [5–7], have also attracted a great deal of attention.

Neutron production is one of the key areas of the field of nuclear reactions in laser-generated plasmas [8–13]. Normally the experimental access to high neutron flux is mainly at large-scale reactor and accelerator-based facilities. However, the development of Petawatt-class laser provides the opportunity of having intense neutron beam generated by comparatively smaller-scale laser facilities [11–13]. The common solution for neutron production in the Petawatt-class laser facilities is via high-energy particle beams interacting with a secondary target, in which the lasers are used for the acceleration of particles [11–13]. In this manner, intense neutron beams with the order of 10^9 – 10^{10} per pulse can be obtained [11–13].

Neutrons produced from thermonuclear reactions in plasmas at a few keV temperatures have a much narrow energy spectrum comparing to the neutrons produced via high-energy ion beams interacting with a secondary target. In this letter, we study the intense neutron beams produced from thermonuclear reactions in laser-generated plasmas. We analyze the reaction ${}^2\text{H}(d, n){}^3\text{He}$ in plasmas generated by Petawatt-class laser interacting with D_2 gas jet targets and CD_2 solid-state

targets. Narrow band-width and intense neutron beams can be obtained from thermonuclear reactions in plasmas generated by Petawatt-class lasers, which are about two orders of magnitude narrower in the neutron-energy bandwidth and reach in the intensity a similar order comparing to the state-of-the-art neutron beams produced in similar laser facilities [12]. Such intense and narrow band-width neutron beams have numerous applications in both industry and fundamental research, such as the interrogation of material and life science [14, 15], nuclear fission and fusion research [16], and neutron capture experiments for fundamental nuclear physics and nuclear astrophysics [17]. The use of CD_2 solid-state targets can enhance the neutron production. In addition, the use of CD_2 solid-state targets can also lead to direct measurements of the reaction rates at low temperatures and great enhancement on the plasma screening comparing to the case of D_2 gas jet targets, offering the possibility to access to these so far unsolved issues in the field of astrophysics [18–30].

We first study the neutron events as functions of plasma temperature adopting a general spherical plasma model, and calculate the neutron spectra. Then we model the plasma formation by the scaling law method for D_2 gas jet targets, and the particle in cell (PIC) method for CD_2 solid-state targets. Plasma screening effects for thermonuclear reactions are discussed in the end to show the astrophysical interests of the present study.

The reactions of interest can be expressed as $n_1 + n_2 \rightarrow n_3 + n_4$, where n_k stands for the number of the nuclear species k . The reaction rates per unit volume are then given by [31]

$$P_{12} = \rho N_A \Lambda_{12 \rightarrow 34}, \quad (1)$$

where ρ is the matter density, N_A is Avogadro number, and $\Lambda_{12 \rightarrow 34} = N_A \langle \sigma v \rangle_{12} Y_1 Y_2 \rho / (n_1!)$, with $Y_k = X_k / A_k$ (X_k is the mass fraction and A_k is the mass number). The total event number N_t is then given by

$$N_t = \int dV dt P_{12}. \quad (2)$$

Assuming a uniform plasma with a spherical shape, the total event number is $N_t = P_{12}V\tau_p$ with the plasma volume V and the plasma lifetime τ_p . The plasma lifetime can be provided by the hydrodynamic expansion [32, 33],

$$\tau_p = R_p \sqrt{m_{\text{ion}}/(T_e Z_{\text{ion}})}, \quad (3)$$

where R_p is the plasma radius, m_{ion} is the ion mass, T_e is the plasma temperature, and Z_{ion} is the ion charge state.

We first consider the reaction ${}^2\text{H}(d, n){}^3\text{He}$ with a Q -value of 3.269 MeV in plasmas generated by D_2 gas jet targets. The highest density of gas jet targets so far is around 10^{21} cm^{-3} [34, 35]. In this case, the plasma volume can be estimated by $V = E_{\text{laser}} f_{\text{abs}}/[T(n_{\text{ion}} + n_e)]$, where E_{laser} is the laser pulse energy and f_{abs} is the total laser absorption fraction. The numbers of the neutron events per laser shot as functions of plasma temperature are shown in Fig. 1, for selected deuterium number densities n_d . A laser pulse with energy $E_{\text{laser}} = 500 \text{ J}$ and the total laser absorption fraction $f_{\text{abs}} = 0.1$ are adopted. The reaction rates of ${}^2\text{H}(d, n){}^3\text{He}$ are adopted from the NACRE II database [31]. As shown in Fig. 1, the neutron events reaches the maximal value $\sim 10^9$ per pulse at temperature $\sim 10 \text{ keV}$.

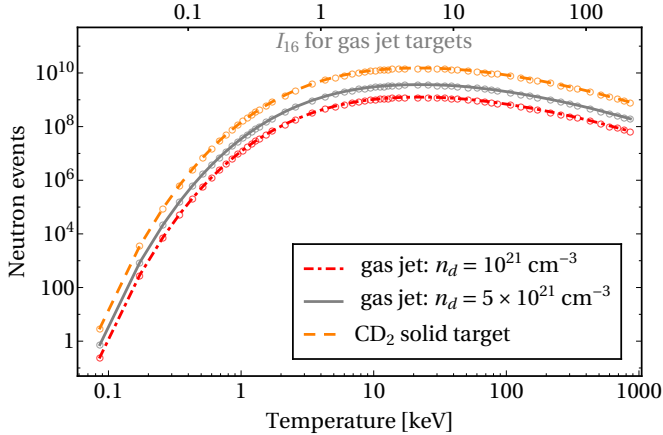


FIG. 1. Neutron events as function of temperature in plasmas generated by D_2 gas jet targets and CD_2 solid-state targets. Here, a laser pulse with energy $E_{\text{laser}} = 500 \text{ J}$ is adopted, and carbon and deuterium ions are assumed to be fully ionized. For gas jet targets, the total laser absorption fraction $f_{\text{abs}} = 0.1$ is adopted. For CD_2 solid-state targets, the total laser absorption fraction $f_{\text{abs}} = 0.2$ are adopted and the carbon number density of the target is $4 \times 10^{22} \text{ cm}^{-3}$. The top frame shows the laser intensity to generate the plasma according to the scaling law, and it is valid for the gas jet case.

These results show that the high density of the target case is more advantageous. In addition, high-density case is of particular interest also in astrophysics, since the density in astrophysical environments is normally extremely high. Therefore, we consider also a CD_2 solid-state target. By adopting the simple spherical plasma model,

we can obtain the neutron events in this case, which are shown also in Fig. 1. Significantly large number of events can be achieved even for temperature around 10^6 K ($\sim 100 \text{ eV}$). This may allow us to make direct measurements of the reaction rates at low temperatures, to avoid the dangers of the extrapolation of the experimental data from the accelerator-based experiments to the energy region of astrophysical interests [2, 18, 31]. We note here that, so far, the lower limit of the c.m.s. energy for the reaction ${}^2\text{H}(d, n){}^3\text{He}$ covered by the experimental data is a few keV [31]. The result also shows that the neutron events reaches the maximal value $\sim 10^{10}$ per pulse at temperature $\sim 10 \text{ keV}$. We note here that the angular distribution of the neutrons produced from thermonuclear reactions is isotropic. If one uses this neutron source as neutron beam with a certain direction, then only part of the neutron can be used. However, the neutron beams produced via laser-induced particle acceleration leading to high-energy particle beams that subsequently interact with a secondary target have also quite large angle divergence or even are isotropic [11–13]. Thus, the intensity of the neutron beams reached here is comparable.

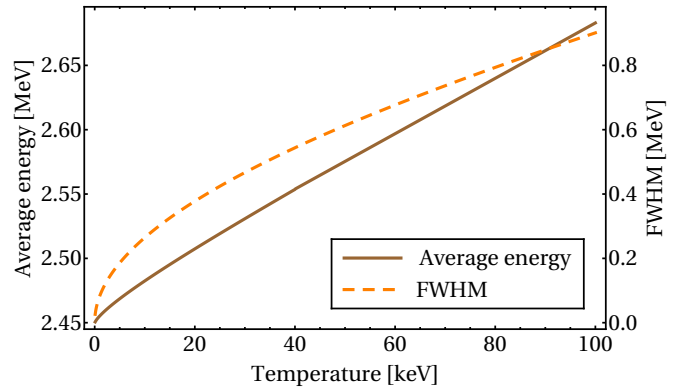


FIG. 2. Average energy (brown solid curve) and FWHM (orange dashed curve) of neutrons produced from the reaction ${}^2\text{H}(d, n){}^3\text{He}$ in plasmas as functions of plasma temperature.

In order to calculate the neutron spectra, we follow the relativistic calculation of fusion product spectra for thermonuclear reactions introduced in Refs. [36, 37]. Based on the relativistic kinematics, one obtains the average energy $\langle E \rangle$ of neutrons produced from the thermonuclear reaction in a plasma [36, 37], $\langle E \rangle = E_0 + \Delta E_{\text{th}}$, where E_0 is the neutron energy at $T = 0$ ($E_0 = 2.4495 \text{ MeV}$ for the reaction under consideration [36, 37]), and ΔE_{th} is the thermal peak shift. The full width at half maximum (FWHM) of the neutron spectra can be described by [36, 37], $W_{1/2} = \omega_0(1 + \delta_\omega)\sqrt{T}$, where ω_0 is the $T \rightarrow 0$ limit for $W_{1/2}/\sqrt{T}$, and $\delta_\omega(T)$ is the correction term. $\omega_0 = 82.542 \text{ keV}^{1/2}$ for the reaction ${}^2\text{H}(d, n){}^3\text{He}$ [36, 37]. Interpolation formulas were obtained [36, 37] for the peak shift ΔE_{th} and the correction term δ_ω for the

width, where the expression

$$\frac{\alpha_1}{1 + \alpha_2 T^{\alpha_3}} T^{2/3} + \alpha_4 T, \quad (4)$$

is valid for $0 < T < 40$ keV, and

$$\alpha_5 + \alpha_6 T, \quad (5)$$

for $30 < T < 100$ keV. The values of the parameters α_i can be found in Refs. [36, 37].

The average neutron energy and FWHM of the neutron spectrum for the reaction ${}^2\text{H}(d, n){}^3\text{He}$ as functions of plasma temperature are shown in Fig. 2. The result shows that for a plasma with temperature of a few keV, the FWHM of the spectrum of the produced neutrons is of the order of 100 keV, which is about two orders of magnitude narrower than the one that neutrons produced via laser-induced particle acceleration leading to high-energy particle beams that subsequently interact with a secondary target [12].

Now we turn to the conditions of the generation the plasmas in laser experiments. For low density cases, i.e., the plasmas generated by D_2 gas jet targets, following a similar way in Refs. [38, 39], we can connect the laser parameter to the result by the scaling law

$$T_e \sim 3.6 I_{16} \lambda_\mu^2 \text{ keV}, \quad (6)$$

where I_{16} is the laser intensity in units of 10^{16} W/cm^2 and λ_μ is the wavelength in microns [40–42]. The result of neutron events from the reaction ${}^2\text{H}(d, n){}^3\text{He}$ in plasmas generated by D_2 gas jet targets is shown in Fig. 1 (see the top frame). Here, a laser wavelength $1.053 \mu\text{m}$ is adopted. It is shown that the laser intensity at a few times of 10^{16} W/cm^2 is favourable for the neutron production in plasmas generated by D_2 gas jet targets. We note here that the scaling law (6) is applied for the non-relativistic case, hence the prediction for high laser intensity ($\sim 10^{18} \text{ W/cm}^2$) should not be precise. However, in the present case we focus on the temperature of a few keV (corresponding to laser intensity in the order of 10^{16} W/cm^2); the result for high laser intensity is shown here for the sake of comparison.

We now turn to the high density case. Experiments and simulations have shown that it is possible to heat targets at solid-state density to temperatures of a few hundred eV or even a few keV [38, 43–45]. Since in this regime the heating of the target is mainly conducted by secondary particles, i.e., hot electrons generated in the laser-target interaction, a more sophisticated model is necessary compared to the low-density case. In order to study plasmas at solid-state density, PIC method is adopted. We have performed a 2-dimensional (2-D) PIC simulation by using the EPOCH code [46]. A CD_2 target with the carbon number density of $4 \times 10^{22} \text{ cm}^{-3}$ is adopted. The thickness of the target is $1 \mu\text{m}$ (x -axis) and the length of the target is $5 \mu\text{m}$ (y -axis). The laser

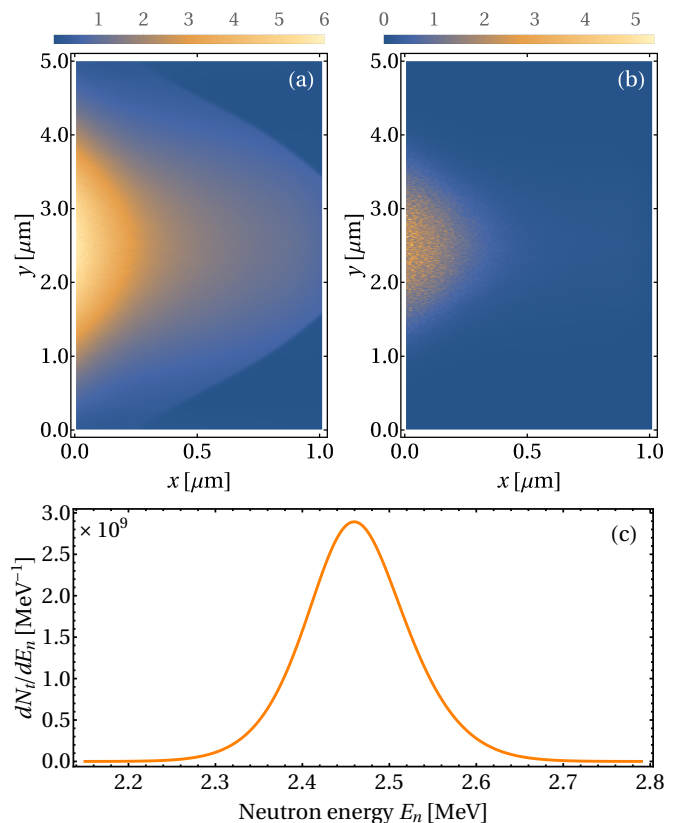


FIG. 3. Results in the solid-target region of the 2-D PIC simulation at time 2.5 ps. (a): Temperature in units of keV. (b): Neutron production rate per unit volume of the reaction ${}^2\text{H}(d, n){}^3\text{He}$ in units of $10^{25} \text{ cm}^{-3} \text{ s}^{-1}$. (c): Neutron distribution (dN_t/dE_n) of neutrons from the reaction ${}^2\text{H}(d, n){}^3\text{He}$. A CD_2 target with the carbon number density of $4 \times 10^{22} \text{ cm}^{-3}$ is adopted, and carbon and deuterium ions are assumed to be fully ionized. The laser has a Gaussian profile in time with a FWHM of 100 fs and a Gaussian profile in the y -axis with a FWHM of $2 \mu\text{m}$. The peak intensity of the laser is 10^{18} W/cm^2 and the laser wavelength is $1.053 \mu\text{m}$. For the neutron distribution (c), a laser pulse energy of 500 J is assumed.

propagates along the x -axis, and it has a Gaussian profile in time with a FWHM of 100 fs and a Gaussian profile in the y -axis centring at the center of the target with a FWHM of $2 \mu\text{m}$. The peak intensity and wavelength of the laser are 10^{18} W/cm^2 and $1.053 \mu\text{m}$, respectively. The size of the simulation box is $4 \mu\text{m} \times 6 \mu\text{m}$, and the target is located at the center of the simulation box. A linear preplasma with thickness $0.5 \mu\text{m}$ is considered in front of the target. Carbon and deuterium ions are assumed to be fully ionized. The electron temperature in the solid-target region at 2.5 ps is shown in Fig. 3(a). It is shown that the target can be heated to a few keV at the solid-state density in the laser focal spot. With such density and temperature, we obtained the neutron production rate per unit volume of the reaction ${}^2\text{H}(d, n){}^3\text{He}$, shown in Fig. 3(b).

By assuming a laser pulse energy of 500 J and estimating the plasma lifetime by the hydrodynamic expansion, we calculate the neutron production events and the neutron spectrum. The neutron distribution (dN_t/dE_n) from the whole solid-target region is shown in Fig. 3(c) as a function of neutron energy E_n . An intense neutron beam with a peak exceeds 10^9 MeV $^{-1}$ is obtained. This reaches a similar order as the state-of-the-art neutron beams produced in similar laser facilities via laser-induced particle acceleration leading to high-energy particle beams that subsequently interact with a secondary target [12, 13]. The advantage of the such an intense neutron beam is that its bandwidth is much narrow.

Comparing with results in Ref. [38], one may expect that lasers with longer duration can heat the target to a higher temperature, which can reach the optimal temperature shown in Fig. 1, leading to a higher number of produced neutrons. In the opposite, it is expected that lasers with shorter duration can heat the target to a lower temperature with astrophysical interests.

As a further advantage, adopting the solid-state target to study nuclear reaction in laser-generated plasmas also allows us to analyze plasma screening effects for thermonuclear reactions [18–30]. Nuclear reactions could be drastically affected inside plasmas, owing to the charge screening effects. Due to the plasma screening effects, the reaction rate can be enhanced by a factor [1], $\langle \sigma v \rangle_{\text{scr}} = g_{\text{scr}} \langle \sigma v \rangle$. In weakly coupled plasmas, i.e., plasmas in which the Coulomb interaction energy between the nucleus and the nearest few electrons and nuclei is small compared to the thermal energy T , the screening enhancement factor is given by [19–21] $g_{\text{scr}} = \exp[Z_1 Z_2 \alpha / (T \lambda_D)]$, where λ_D is the Debye length, α is the fine-structure constant, and Z_1 and Z_2 are the nuclear charges of the reactants. The result for the plasma screening enhancement factor the reaction ${}^2\text{H}(d, n){}^3\text{He}$ calculated by the week screening as functions of plasma temperature in plasmas generated by D_2 gas jet targets is shown in Fig. 4, for the case of deuterium number density $n_d = 10^{21}$ cm $^{-3}$. It is shown that the plasma screening effect for the reaction ${}^2\text{H}(d, n){}^3\text{He}$ in plasmas generated by D_2 gas jet targets is basically negligible. However, the plasma effect is greatly enhanced in the case of CD_2 solid-state targets, as shown in Fig. 4. As the neutron events are large enough for low temperatures in the case of CD_2 targets shown in Fig. 1, it may lead to the possible of the direct measurement of plasma screening effects for thermonuclear reactions.

Furthermore, since the density of the CD_2 target is quite high, the low temperature plasma generated by the target may reached the condition for strong screening [19], $Z_1 < \rho^{1/3}$ and $0.23 Z_1^{2/3} z(\xi \rho)^{1/3} T_6^{-1} > 1$, where for the case of CD_2 plasma with temperature $\sim 10^6$ K (~ 100 eV), $0.23 Z_1^{2/3} z(\xi \rho)^{1/3} T_6^{-1} \sim 1$. Here ξ is given by $\xi = \sum_i (X_i Z_i) / A_i$ and T_6 stands for the

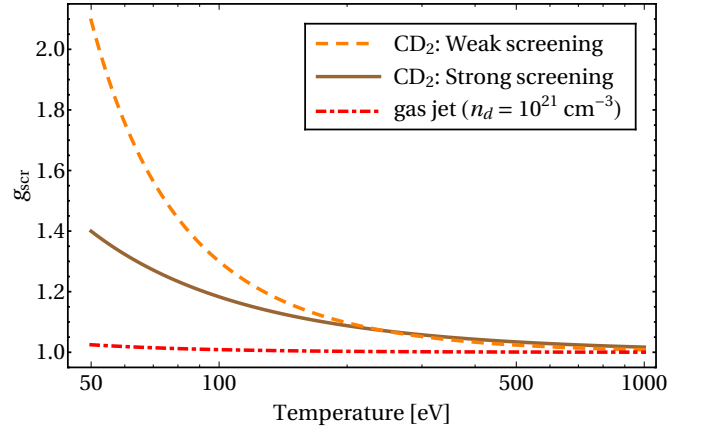


FIG. 4. Plasma screening enhancement factor (weak-screening) for the reaction ${}^2\text{H}(d, n){}^3\text{He}$ as a function of plasma temperature in plasmas generated by D_2 gas jet targets with $n_d = 10^{21}$ cm $^{-3}$ (red dot-dashed curve), and plasma screening enhancement factor (weak-screening: orange dashed curve, strong-screening: brown solid curve) for the reaction ${}^2\text{H}(d, n){}^3\text{He}$ in plasmas generated by CD_2 solid-state targets. Carbon and deuterium ions are assumed to be fully ionized. For the case of CD_2 solid-state target, the carbon number density of the target is 4×10^{22} cm $^{-3}$.

plasma temperature in units of 10^6 K. In this case, the plasma screening enhancement factor is given by $g_{\text{scr}} = \exp\left\{0.205 \left[(Z_1 + Z_2)^{5/3} - Z_1^{5/3} - Z_2^{5/3}\right] (\xi \rho)^{1/3} T_6^{-1}\right\}$. The strong screening enhancement factor for the case of CD_2 solid-state target is also shown in Fig. 4 as a function of plasma temperature. For temperature of $\sim 10^6$ K, the strong screening enhancement factor is significantly different from the weak screening one, which could lead to the experimental determination of the strong screening effect for fusion reactions in plasmas.

In conclusion, we have studied the intense neutron beams produced from thermonuclear reactions in laser-generated plasmas. The reaction ${}^2\text{H}(d, n){}^3\text{He}$ in plasmas generated by Petawatt-class laser interacting with D_2 gas jet targets and CD_2 solid-state targets has been analyzed. We have shown that neutron beams of similar intensity and about two orders of magnitude narrower bandwidth can be obtained from thermonuclear reactions in plasmas generated by Petawatt-class lasers, as comparing with the state-of-the-art neutron beams produced via laser-induced particle acceleration leading to high-energy particle beams that subsequently interact with a secondary target [12, 13]. We have shown also the advantages of the use of CD_2 solid-state targets in the study of thermonuclear reactions for the astrophysical interests, i.e., direct measurements of the reaction rates at low temperatures of nucleosynthesis-relevant energies and great enhancement on the plasma screening comparing to the case of D_2 gas jet targets, opening new possibilities to study these so far unsolved issues in astrophysics.

We thank Adriana Pálffy and Christoph H. Keitel for fruitful discussions.

* yuanbin.wu@mpi-hd.mpg.de

- [1] S. Atzeni and J. Meyer-ter Vehn, *The Physics of Inertial Fusion: Beam-Plasma Interaction, Hydrodynamics, Hot Dense Matter* (Oxford University Press, Oxford, 2004).
- [2] F. Negoita, M. Roth, P. G. Thirolf, S. Tudisco, F. Hannachi, S. Moustazis, I. Pomerantz, P. McKenna, J. Fuchs, K. Sphor, et al., *Romanian Reports in Physics* **68**, **Supplement**, S37 (2016).
- [3] D. T. Casey, J. A. Frenje, M. Gatu Johnson, M. J.-E. Manuel, N. Sinenian, A. B. Zylstra, F. H. Séguin, C. K. Li, R. D. Petrasso, V. Y. Glebov, et al., *Phys. Rev. Lett.* **109**, 025003 (2012).
- [4] A. B. Zylstra, H. W. Herrmann, M. G. Johnson, Y. H. Kim, J. A. Frenje, G. Hale, C. K. Li, M. Rubery, M. Paris, A. Bacher, et al., *Phys. Rev. Lett.* **117**, 035002 (2016).
- [5] C. J. Cerjan, L. Bernstein, L. Berzak Hopkins, R. M. Bionta, D. L. Bleuel, J. A. Caggiano, W. S. Cassata, C. R. Brune, D. Fittinghoff, J. Frenje, et al., *Journal of Physics G: Nuclear and Particle Physics* **45**, 033003 (2018).
- [6] O. A. Hurricane, D. A. Callahan, D. T. Casey, P. M. Celliers, C. Cerjan, E. L. Dewald, T. R. Dittrich, T. Döppner, D. E. Hinkel, L. F. Berzak Hopkins, et al., *Nature* **506**, 343 (2014).
- [7] R. E. Olson, R. J. Leeper, J. L. Kline, A. B. Zylstra, S. A. Yi, J. Biener, T. Braun, B. J. Kozioziemski, J. D. Sater, P. A. Bradley, et al., *Phys. Rev. Lett.* **117**, 245001 (2016).
- [8] T. Ma, O. A. Hurricane, D. A. Callahan, M. A. Barrios, D. T. Casey, E. L. Dewald, T. R. Dittrich, T. Döppner, S. W. Haan, D. E. Hinkel, et al., *Phys. Rev. Lett.* **114**, 145004 (2015).
- [9] T. Döppner, D. A. Callahan, O. A. Hurricane, D. E. Hinkel, T. Ma, H.-S. Park, L. F. Berzak Hopkins, D. T. Casey, P. Celliers, E. L. Dewald, et al., *Phys. Rev. Lett.* **115**, 055001 (2015).
- [10] T. Ditmire, J. Zweiback, V. P. Yanovsky, T. E. Cowan, G. Hays, and K. B. Wharton, *Nature* **398**, 489 (1999).
- [11] D. P. Higginson, L. Vassura, M. M. Gugi, P. Antici, M. Borghesi, S. Brauckmann, C. Diouf, A. Green, L. Palumbo, H. Petrascu, et al., *Phys. Rev. Lett.* **115**, 054802 (2015).
- [12] M. Roth, D. Jung, K. Falk, N. Guler, O. Deppert, M. Devlin, A. Favalli, J. Fernandez, D. Gautier, M. Geissel, et al., *Phys. Rev. Lett.* **110**, 044802 (2013).
- [13] I. Pomerantz, E. McCary, A. R. Meadows, A. Arefiev, A. C. Bernstein, C. Chester, J. Cortez, M. E. Donovan, G. Dyer, E. W. Gaul, et al., *Phys. Rev. Lett.* **113**, 184801 (2014).
- [14] G. Zaccai, *Science* **288**, 1604 (2000).
- [15] J. Ma, O. Delaire, A. F. May, C. E. Carlton, M. A. McGuire, L. H. VanBebber, D. L. Abernathy, G. Ehlers, T. Hong, A. Huq, et al., *Nature Nanotechnology* **8**, 445 (2013).
- [16] L. J. Perkins, B. G. Logan, M. D. Rosen, M. D. Perry, T. Diaz de la Rubia, N. M. Ghoniem, T. Ditmire, P. T. Springer, and S. C. Wilks, *Nuclear Fusion* **40**, 1 (2000).
- [17] D. L. Bleuel, L. A. Bernstein, C. A. Brand, W. S. Cassata, B. H. Daub, L. S. Dauffy, B. L. Goldblum, J. M. Hall, C. A. Hagmann, L. Berzak Hopkins, et al., *Plasma and Fusion Research* **11**, 3401075 (2016).
- [18] E. G. Adelberger, A. García, R. G. H. Robertson, K. A. Snover, A. B. Balantekin, K. Heeger, M. J. Ramsey-Musolf, D. Bemmerer, A. Junghans, C. A. Bertulani, et al., *Rev. Mod. Phys.* **83**, 195 (2011).
- [19] E. E. Salpeter, *Australian Journal of Physics* **7**, 373 (1954).
- [20] A. V. Gruzinov and J. Bahcall, *The Astrophysical Journal* **504**, 996 (1998).
- [21] Y. Wu and A. Pálffy, *The Astrophysical Journal* **838**, 55 (2017).
- [22] G. Keller, *The Astrophysical Journal* **118**, 142 (1953).
- [23] E. E. Salpeter and H. M. Van Horn, *The Astrophysical Journal* **155**, 183 (1969).
- [24] H. C. Graboske, H. E. Dewitt, A. S. Grossman, and M. S. Cooper, *The Astrophysical Journal* **181**, 457 (1973).
- [25] H. Dzitzko, S. Turck-Chièze, P. Delbourgo-Salvador, and C. Lagrange, *The Astrophysical Journal* **447**, 428 (1995).
- [26] J. N. Bahcall, L. S. Brown, A. Gruzinov, and R. F. Sawyer, *Astronomy & Astrophysics* **383**, 291 (2002).
- [27] S. M. Chitanvis, *The Astrophysical Journal* **654**, 693 (2007).
- [28] N. J. Shaviv and G. Shaviv, *The Astrophysical Journal* **486**, 433 (1996).
- [29] G. Shaviv and N. J. Shaviv, *The Astrophysical Journal* **529**, 1054 (2000).
- [30] D. Mao, K. Mussack, and W. Däppen, *The Astrophysical Journal* **701**, 1204 (2009).
- [31] Y. Xu, K. Takahashi, S. Goriely, M. Arnould, M. Ohta, and H. Utsunomiya, *Nuclear Physics A* **918**, 61 (2013).
- [32] V. P. Krainov and M. B. Smirnov, *Physics Reports* **370**, 237 (2002).
- [33] J. Gunst, Y. Wu, N. Kumar, C. H. Keitel, and A. Pálffy, *Physics of Plasmas* **22**, 112706 (2015).
- [34] K. Schmid and L. Veisz, *Review of Scientific Instruments* **83**, 053304 (2012).
- [35] F. Sylla, M. Veltcheva, S. Kahaly, A. Flacco, and V. Malka, *Review of Scientific Instruments* **83**, 033507 (2012).
- [36] L. Ballabio, G. Gorini, and J. Källne, *Review of Scientific Instruments* **68**, 585 (1997).
- [37] L. Ballabio, J. Källne, and G. Gorini, *Nuclear Fusion* **38**, 1723 (1998).
- [38] Y. Wu, J. Gunst, C. H. Keitel, and A. Pálffy, *Phys. Rev. Lett.* **120**, 052504 (2018).
- [39] J. Gunst, Y. Wu, C. H. Keitel, and A. Pálffy, *Phys. Rev. E* **97**, 063205 (2018).
- [40] F. Brunel, *Phys. Rev. Lett.* **59**, 52 (1987).
- [41] G. Bonnaud, P. Gibbon, J. Kindel, and E. Williams, *Laser and Particle Beams* **9**, 339 (1991).
- [42] P. Gibbon and E. Förster, *Plasma Physics and Controlled Fusion* **38**, 769 (1996).
- [43] A. Saemann, K. Eidmann, I. E. Golovkin, R. C. Mancini, E. Andersson, E. Förster, and K. Witte, *Phys. Rev. Lett.* **82**, 4843 (1999).
- [44] P. Audebert, R. Shepherd, K. B. Fournier, O. Peyrusse, D. Price, R. Lee, P. Springer, J.-C. Gauthier, and L. Klein, *Phys. Rev. Lett.* **89**, 265001 (2002).
- [45] Y. Sentoku, A. J. Kemp, R. Presura, M. S. Bakeman, and T. E. Cowan, *Physics of Plasmas* **14**, 122701 (2007).

- [46] T. D. Arber, K. Bennett, C. S. Brady, A. Lawrence-Douglas, M. G. Ramsay, N. J. Sircombe, P. Gillies, R. G. Evans, H. Schmitz, A. R. Bell, et al., Plasma Physics and Controlled Fusion **57**, 113001 (2015).